MRS Communications (2012), *2*, 107–111
© Materials Research Society, 2012
doi:10.1557/mrc.2012.18

MRS Communications

Research Letters

Improved oxygen surface exchange kinetics at grain boundaries in nanocrystalline yttria-stabilized zirconia

Joong Sun Park, Department of Mechanical Engineering, Stanford University, Stanford, California 94305; Environmental Energy Technologies Division, Lawrence Berkeley National Laboratory, Berkeley, California 94720
Timothy P. Holme, Department of Mechanical Engineering, Stanford University, Stanford, California 94305
Joon Hyung Shim, Department of Mechanical Engineering, Stanford University, Stanford, California 94305; Department of Mechanical Engineering, Korea University, Seoul, Korea
Fritz B. Prinz, Department of Mechanical Engineering, Stanford University, Stanford, California 94305; Department of Material Science and Engineering, Stanford University, Stanford, California 94305

Address all correspondence to Joong Sun Park at **joongspark@lbl.gov**

(Received 28 March 2012; accepted 30 July 2012)

Abstract

Quantum simulations of oxygen incorporation at a Σ5 grain boundary in yttria-stabilized zirconia (YSZ), a common solid oxide fuel cells (SOFCs) electrolyte, show that the incorporation energy is reduced compared with YSZ with no grain boundaries. The simulation results are supported by electrochemical impedance spectroscopy (EIS) measurements conducted on a single crystalline YSZ substrate with nanogranular interlayered YSZ. EIS results showed that single crystalline YSZ membranes with nanogranular surface (i.e., high grain boundary densities) exhibit small electrode impedances than the reference single crystalline YSZ. The 20-nm-thick nanogranular YSZ interlayer was fabricated by atomic layer deposition and the performance for SOFCs with nanograined interlayer was increased by factor of 2 at operating temperatures between 350 and 450 °C.

Acceptor-doped cubic fluorite structures such as doped zirconia and ceria have been widely investigated as oxide ion conductors, which can be applicable to oxygen sensors or electrolytes for solid oxide fuel cells (SOFCs). Among those materials, yttria-stabilized zirconia (YSZ) is of most interest because of its high ionic conductivity combined with chemical stability. Recently, those materials have shown superior properties when they are synthesized at the nanoscale.[1–2] Knoner et al.[1] reported that ionic conductivity is significantly enhanced in nanocrystalline YSZ. The conductivity seems related to structural characteristics, i.e., increased grain boundaries that are loosely packed where vacancy-type free volume forms. Huang et al.[3] has also demonstrated enhanced ionic conduction in gadolinia-doped ceria (GDC) when it is fabricated at the nanoscale due to reduction of number of blocking grain boundaries perpendicular to ion motion, which greatly impede ion transport across them.

Our group has recently succeeded in fabrication of low-temperature SOFCs equipped with 65-nm-thick YSZ electrolytes by atomic layer deposition (ALD) techniques.[4] The performance of those fuel cells has been improved at low temperatures due to reduction of electrolyte thickness. Interestingly, SOFC with ALD YSZ films has been measured to have greatly enhanced surface exchange current density, a purely surface phenomenon. Recent high spatial resolution secondary mass spectrometry (NanoSIMS) study combined with electrochemical impedance spectroscopy (EIS) showed that high grain boundary densities at the surface of YSZ improved the oxygen reduction reaction (ORR),[5] and it implies that the enhanced exchange current density in ALD YSZ SOFC may result from the nanogranular structure of the film. In the present study, we performed ab initio simulation of oxygen incorporation in YSZ at a grain surface and at a Σ5 grain boundary to study the role of grain boundaries in oxygen incorporation. In addition, we experimentally investigated the role of the thin nanocrystalline YSZ layer on a single crystalline YSZ substrate and correlate computation results to the performances of the fuel cells with a nanocrystalline layer at the cathode side.

To gain insight into energetics of oxygen surface kinetics on YSZ, the energy pathway for oxygen incorporation at a grain boundary in YSZ was calculated using periodic boundary condition density functional theory (DFT) as implemented by Vienna Ab-initio Simulation Package (VASP).[6] Electron wavefunctions were expanded in a plane-wave basis set up to a cutoff of 400 eV using projector-augmented waves[7] with the Ceperley–Alder exchange-correlation functional as parameterized by Perdew and Zunger[8] with relativistic corrections. Gaussian smearing was used with a width of 0.2 eV to determine partial occupancies. Energy was sampled on a $2 \times 2 \times 1$

https://doi.org/10.1557/mrc.2012.18 Published online by Cambridge University Press

Monkhorst–Pack[9] lattice of *k*-points. The electronic self-consistent charge density was computed to a tolerance of 10^{-4} eV.

The supercell is composed of 3 × 3 × 3 unit cells of YSZ of stoichiometry $(ZrO_2)_{23}(Y_2O_3)_2$ (8 mol% YSZ) and 17 Å vacuum separation of adjacent slabs. The grain boundary chosen for this system is a Σ5 grain boundary derived from coincident site lattice theory. To create the grain boundary, half of the YSZ slab is rotated by 36.9° to obtain two grain boundaries: one in the center of the slab and one at the boundary of the supercell. As a result of the rotation, some ions from the right half of the slab lie in the left crystal grain (and vice versa); these ions are removed and full relaxation is allowed. After relaxation, the mean displacement of atoms in the supercell is 0.43 Å and the maximum displacement is 2.6 Å, indicating that rather large rearrangements occur.

The results of DFT calculations of atomic oxygen incorporation at a Σ5 grain boundary and in a system with no grain boundary are presented in Fig. 1. Oxygen adsorption enthalpy is −2.80 and −0.23 eV on the YSZ surface with no grain boundary and Σ5 grain boundary, respectively. A possible explanation for why it is more favorable for oxygen to adsorb on the crystalline surface is that, as in epitaxy, the oxygen will tend to sit near a low-energy site of a virtual additional layer, whereas at a grain boundary no such virtual site is defined.

Incorporation into a surface vacancy with no grain boundary is an activated process with $E_a = 0.26$ eV, while incorporation at a grain boundary has no activation energy. In both cases, the final state of incorporation is downhill from the adsorbed state, by 0.40 and 0.36 eV for a grain boundary and in a single crystal, respectively. We postulate that a higher vacancy concentration at a grain boundary allows the atoms to rearrange at a lower energy cost than in a single crystal, explaining why the energy barrier for incorporation is lower near a grain boundary. This result agrees with an experimental study from our laboratory reported earlier.[10] The simulation assumes that the oxygen has dissociated from molecular oxygen to atomic oxygen. If the grain boundary is near a catalyst, this

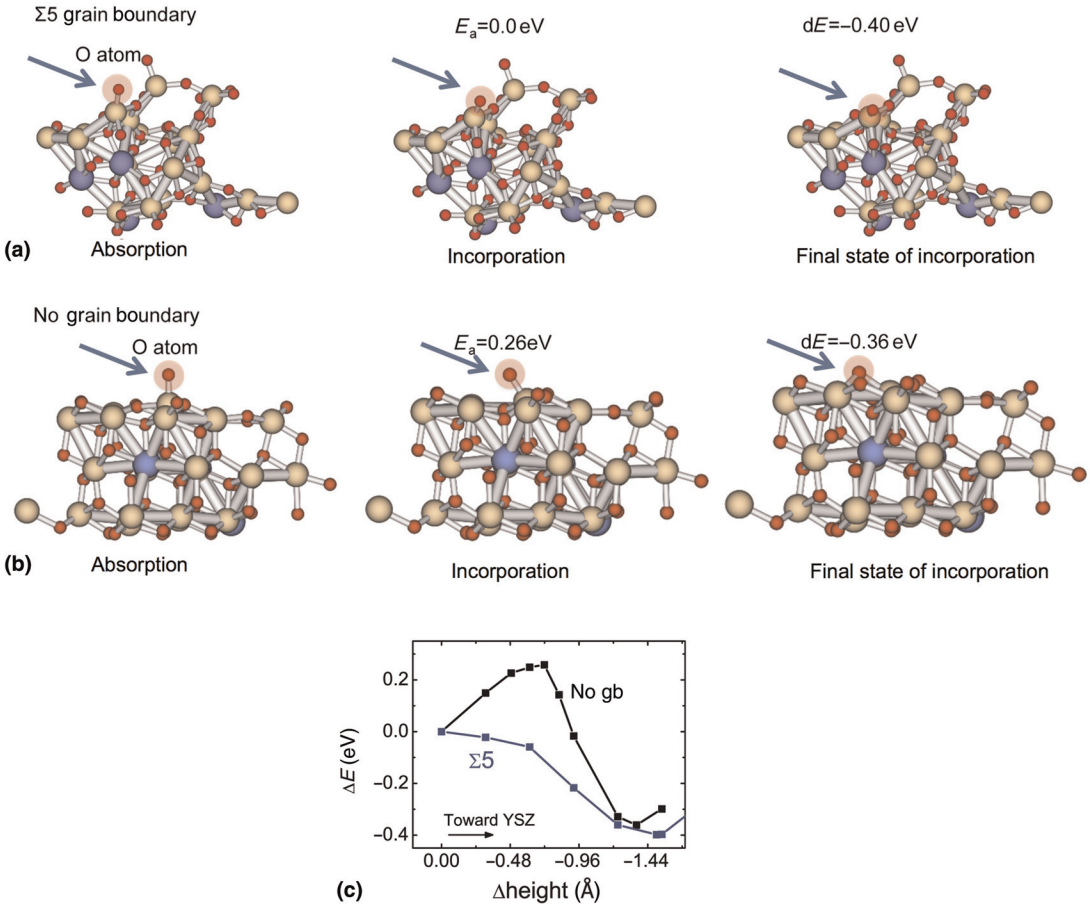


Figure 1. Incorporation of atomic oxygen in YSZ (a) with a Σ5 grain boundary and (b) without a grain boundary. Red circles indicate the diffusing oxygen. Oxygen atoms are shown in red, Zr in brown and Y in blue. (c) Change in energy during incorporation versus oxygen height (both are in terms of the difference from the adsorbed state). The height is measured in Å from the height (*z*-coordinate) of oxygen adsorbed on the surface of the YSZ to the height (*z*-coordinate) of oxygen as it moves down into a surface vacancy position. The caption states that the height is a difference from the adsorbed state.

https://doi.org/10.1557/mrc.2012.18 Published online by Cambridge University Press

dissociation may occur on the catalyst particle and the dissociated oxygen may diffuse along the YSZ surface to reach a grain boundary, where incorporation is favorable. Therefore, grain boundary engineering may be a particularly beneficial way to profit from the spillover effect.[11]

To correlate quantum simulation results with the electrochemical performances of fuel cells, we fabricated fuel cells with nanogranular surface by ALD, and characterized impedances during ORR. For this purpose, a 500-μm-thick polished single crystalline YSZ (100) Marketech Inc. (Port Townsend, WA) were loaded into a custom-built, flow-type ALD system for YSZ thin films described elsewhere.[4] Fabricated ALD YSZ films were characterized by atomic force microscopy (AFM) and average grain size is measured to 20–30 nm. Accordingly, the sample does not have grain boundaries in the bulk but granular structures only at the surface. Interfacial impedance and conductivity measurements were made using EIS in the temperature range of 350–450 °C at 50 °C intervals for samples with and without surface nanogranular layer. The frequency range for EIS measurements was from 0.1 Hz to 100 kHz. Porous platinum was deposited on both sides of the YSZ by d.c. sputtering at an Ar pressure of 10 Pa. All samples used in this study were loaded together for deposition to eliminate the variation in thickness and uniformity among samples. The morphologies of sputtered platinum were studied using AFM and scanning electron microscopy (SEM), and it showed little differences in platinum morphologies between the samples. SOFCs were measured with the anode exposed to pure hydrogen (10 sccm) and the cathode exposed to the air. SEM morphologies of two samples before and after SOFC measurements were observed with little difference as shown in Fig. 2. In spite of the morphological changes due to Ostwald ripening after a thermal cycle, which led to microstructural coarsening, in both samples, the microstructure of the two samples was not affected by the underlying substrate, yielding similar porous structures.

Figure 3 shows the EIS spectra of the nanogranular interlayered sample and the reference YSZ sample at the temperature windows between 350 and 450 °C. There are two distinct semi-circles where high-frequency loops indicate electrolyte impedance and low-frequency loops correspond to electrode process. The electrolyte impedances, as expected, were not significantly changed by the additional nanogranular YSZ interlayer, because the ohmic loss caused by 20 nm ALD YSZ thin film was negligible compared with that of 500 μm bulk YSZ electrolyte. However, interface impedances were significantly reduced by the ALD YSZ thin film. It can be concluded that this reduction mainly came from the cathode/electrolyte interface as ALD YSZ film was deposited only on the cathode side. The electrode impedance mainly comes from two individual electrochemical reactions, namely hydrogen oxidation reaction (HOR) and ORR during SOFC operation. It is commonly known that the ORR is more sluggish than the HOR.[12–14] In addition, the reaction area for the anode is more than 10 times larger than the cathode active area. Therefore, we can conclude that the small anode semi-circle is merged into the cathodic semi-circle, and it can be concluded that changes in the low-frequency impedance loop (for

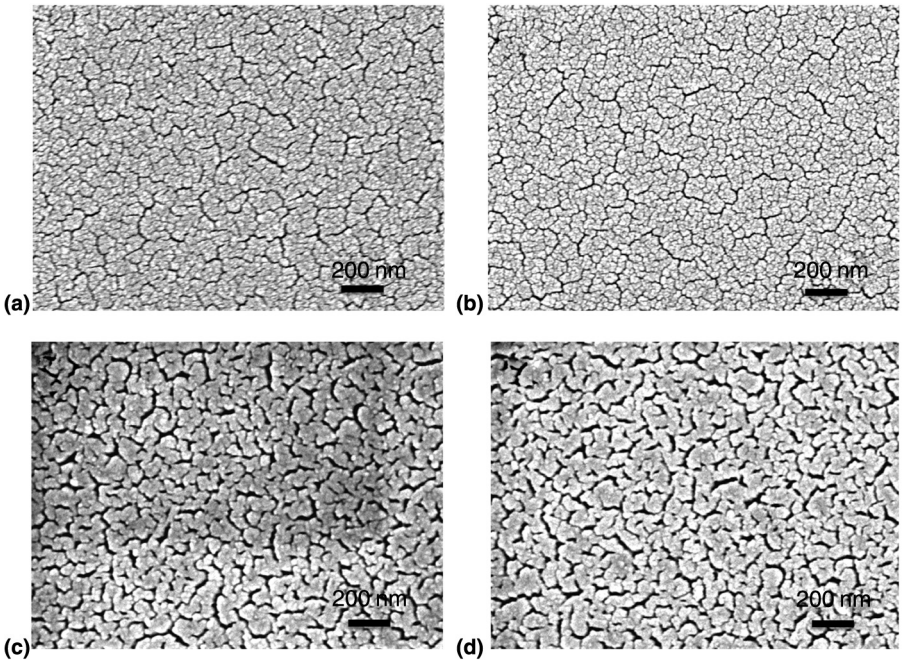


Figure 2. SEM images of platinum morphologies on (a), (b) single crystalline YSZ and nanogranular interlayer before SOFC measurement, (c), (d) single crystalline YSZ and nanogranular interlayer after SOFC measurement.

https://doi.org/10.1557/mrc.2012.18 Published online by Cambridge University Press

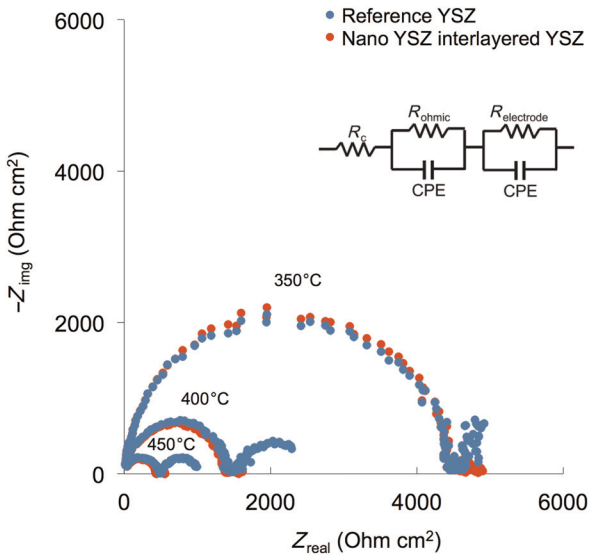


Figure 3. EIS spectra for SOFCs with and without nanograined interlayer at the cathode at 0.8 V with respect to a counter electrode connected to the anode. High-frequency semi-circle corresponds to a diffusion process in the electrolyte, and low-frequency semi-circle corresponds to interfacial reactions at the electrode/electrolyte.

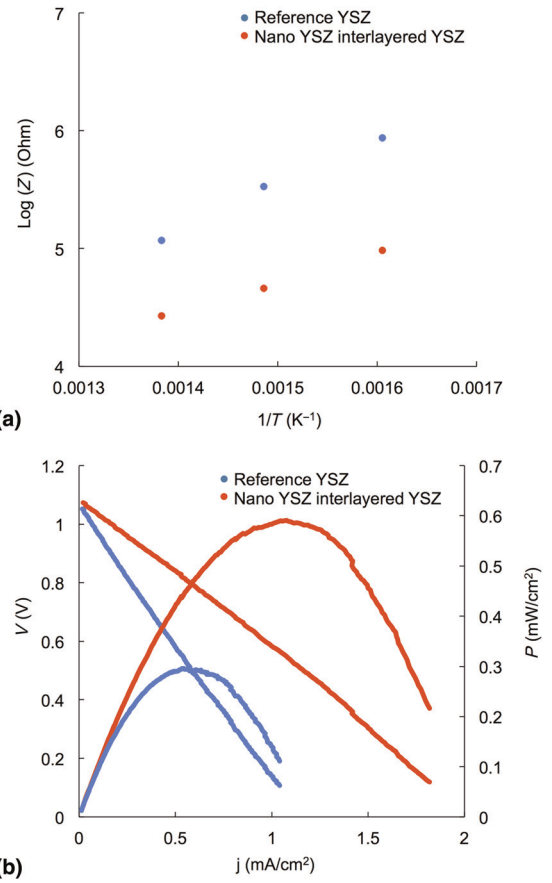


Figure 4. (a) Arrhenius plot of cathodic impedances of samples measured at a cell voltage of 0.8 V at 350–450 °C using EIS, and (b) current–voltage characteristic for SOFCs with and without nanograined interlayer at the cathode at 450 °C.

different samples at the same temperature and cell voltage) are due to the differences in the YSZ electrolyte surface microstructure at the cathode side.

The EIS results were analyzed using Z-plot software based on complex nonlinear least-squares fitting with two parallel resistance-constant phase element, and series resistance.[15] Figure 4(a) shows the Arrhenius plot of the cathodic impedance values at d.c. bias voltage of 0.8 V with respect to a counter electrode connected to the anode. The cathodic impedance of the sample with nanogranular interlayer was approximately 10–15% that of the reference single crystalline sample, suggesting that high densities of grain boundary at the surface enhance oxygen surface exchange and incorporation. The activation energies for the ORR were calculated to be 0.72, 0.46 eV for the single crystalline sample and nanogranular interlayered sample, respectively. These results support DFT simulation results showing the fact that oxygen incorporation at a grain boundary is more energetically favorable than at grain surfaces.

One theory explaining why improved performance is found in samples with nanograined surface points to interface roughness as higher surface roughness can provide additional reaction sites. To study the morphology of surface roughness generated in this manner, we examined the sample surface with AFM. An AFM topography scan showed that there is little difference in RMS roughness between reference single crystalline YSZ (1.5–2 nm) and ALD YSZ-deposited sample (~2 nm). The AFM topography image of the ALD YSZ surface also confirmed that the average grain size is tens of nanometers, showing nanograined surface. Therefore, we can rule out a potential contribution from surface roughness, and interpret the significant reduction in cathodic impedance as an effect of the high grain boundary densities at the surface.

From *I–V* measurements of SOFCs with and without surface-modified layers on the cathode side, it is clear that the nanogranular surface at cathode enhanced the performances of fuel cells as shown in Fig. 4(b). Open-circuit voltages (OCVs) of the nanogranular interlayered fuel cells were measured in the range from 1.05 to 1.07 V, close to the ones measured with reference YSZ (1.03–1.05 V). We observed a significant enhancement of maximum power density in fuel cells with an introduction of 20-nm-thick nanogranular ALD YSZ layer. The maximum power densities at 450 °C of the fuel cells increased twofold with a 20 nm ALD YSZ interlayer, which has high grain boundary densities at the surface. A high density of grain boundary at the surface region increases the vacancy density near the electrode–electrolyte interface, which is likely to enhance the rate of forward reaction of oxygen incorporation into the electrolyte, and this ultimately reduces activation loss during fuel cell operations. These experimental results are in agreement with our previous studies

https://doi.org/10.1557/mrc.2012.18 Published online by Cambridge University Press

showing enhanced oxygen surface exchange and incorporation rate at grain boundaries in YSZ and YDC.[5,16]

In summary, quantum simulations of oxygen incorporation at grain boundaries of YSZ show that grain boundaries, simulated by a Σ5 grain boundary, are more active for atomic O incorporation than grain centers. This result is in accordance with experimental results, which show a significant reduction in the cathode impedance by introducing a nanogranular interlayer. The implications of this study are that activity at the electrolyte/electrode interfaces can be enhanced by having a higher density of grain boundaries.

Acknowledgments

The authors would like to thank Dr. Turgut M. Gür for helpful discussion, and the members of Nanoscale Prototyping Laboratory at Stanford University for their support and suggestions. This research used resources of the National Energy Research Scientific Computing Center, which is supported by the Office of Science of the U.S. Department of Energy under Contract No. DE-AC02-05CH11231.

References

1. G. Knoner, K. Reimann, R. Rower, U. Sodervall, and H.E. Schaeffer: Enhanced oxygen diffusivity in interfaces of nanocrystalline $ZrO_2{\cdot}Y_2O_3$. *Proc. Natl. Acad. Sci. U.S.A.* **100**, 3860 (2003).
2. I. Kosacki, C.M. Rouleau, P.F. Becher, J. Bentley, and D.H. Lowndesb: Surface/interface-related conductivity in nanometer thick YSZ films. *Electrochem. Solid State Lett.* **7**, A459 (2004).
3. H. Huang, T.M. Gür, Y. Saito, and F.B. Prinz: High ionic conductivity in ultrathin nanocrystalline gadolinia-doped ceria films. *Appl. Phys. Lett.* **89**, 143107 (2006).
4. J.H. Shim, C.C. Chao, H. Huang, and F.B. Prinz: Atomic layer deposition of yttria-stabilized zirconia for solid oxide fuel cells. *Chem. Mater.* **19**, 3850 (2007).
5. J.H. Shim, J.S. Park, T.P. Holme, K. Crabb, W. Lee, Y.B. Kim, X. Tian, T.M. Gür, and F.B. Prinz: Enhanced oxygen exchange and incorporation at surface grain boundaries on an oxide ion conductor. *Acta Mater.* **60**, 1 (2012).
6. G. Kresse and J. Furthmüller: Efficient iterative schemes for ab initio total-energy calculations using a plane-wave basis set. *Phys. Rev. B* **54**, 11169 (1996).
7. G. Kresse and J. Joubert: From ultrasoft pseudopotentials to the projector augmented-wave method. *J. Phys. Rev. B* **59**, 1758 (1999).
8. J. Perdew and A. Zunger: Density-functional approximation for the correlation energy of the inhomogeneous electron gas. *Phys. Rev. B* **23**, 5048 (1982).
9. H.J. Monkhorst and J.D. Pack: Special pointes for Brillouin-zone integrations. *Phys. Rev. B* **13**, 5188 (1976).
10. W. Lee, H.J. Jung, M. Lee, Y. Kim, J.S. Park, R. Sinclair, and F.B. Prinz: Oxygen surface exchange at grain boundaries of oxide ion conductors. *Adv. Funct. Mater.* **22**, 965 (2012).
11. W.C. Conner and J.L. Falconer: Spillover in heterogeneous catalysis. *Chem. Rev.* **95**, 759 (1995).
12. H. Huang, M. Nakamura, P. Su, R. Fasching, Y. Saito, and F.B. Prinz: High-performance ultrathin solid oxide fuel cells for low-temperature operation. *J. Electrochem. Soc.* **154**, B20 (2007).
13. S. Souza, S.J. Visco, and L.C. De Jonghe: Thin-film solid oxide fuel cell with high performance at low-temperature. *Solid State Ionics* **98**, 57 (1997).
14. T.P. Holme, R. Pornprasertsuk, and F. Prinz: Interpretation of low temperature solid oxide fuel cell electrochemical impedance spectra. *J. Electrochem. Soc.* **157**, B64 (2010).
15. Y. Kim, T. Holme, T.M. Gür, and F.B. Prinz: Surface-modified low-temperature solid oxide fuel cell. *Adv. Funct. Mater.* **21**, 4684 (2011).
16. Y. Kim, J.S. Park, T.M. Gür, and F.B. Prinz: Oxygen activation over engineered surface grains on YDC/YSZ interlayered composite electrolyte for LT-SOFC. *J. Power Sources* **196**, 19550 (2011).

https://doi.org/10.1557/mrc.2012.18 Published online by Cambridge University Press